

See discussions, stats, and author profiles for this publication at: <https://www.researchgate.net/publication/353737711>

In Silico Analysis of Potential Antidiabetic Phytochemicals from *Matricaria chamomilla* L. against PTP1B and Aldose Reductase for Type 2 Diabetes Mellitus and its Complications

Article in *Natural Product Sciences* · August 2021

DOI: 10.20307/nps.2021.27.2.99

CITATIONS

5

READS

523

6 authors, including:



Arisvia Sukma Hariftyani

Airlangga University

7 PUBLICATIONS 16 CITATIONS

SEE PROFILE



Siti Khaerunnisa

Airlangga University

38 PUBLICATIONS 427 CITATIONS

SEE PROFILE



Rizki Awaluddin

University of Darussalam Gontor

13 PUBLICATIONS 394 CITATIONS

SEE PROFILE

Some of the authors of this publication are also working on these related projects:



Molecular Docking, ADME-Toxicity Prediction, and Evaluation of Curcumin Derivative Compound as Inhibitor Inflammation on Rheumatoid Arthritis [View project](#)



Meta-analysis and Systematic Review of COVID19 [View project](#)



In Silico Analysis of Potential Antidiabetic Phytochemicals from *Matricaria chamomilla* L. against PTP1B and Aldose Reductase for Type 2 Diabetes Mellitus and its Complications

Arisvia Sukma Hariftyani¹, Lady Aqnes Kurniawati¹, Siti Khaerunnisa^{2,*}, Anna Surgean Veterini³, Yuani Setiawati⁴, and Rizki Awaluddin⁵

¹Faculty of Medicine, Universitas Airlangga, Surabaya, Indonesia

²Department of Physiology and Medical Biochemistry, Faculty of Medicine, Universitas Airlangga, Surabaya, Indonesia

³Department of Anesthesiology and Intensive Care, Faculty of Medicine, Universitas Airlangga – Dr. Soetomo General Hospital, Surabaya, Indonesia

⁴Department of Anatomy-Histology and Pharmacology, Faculty of Medicine, Universitas Airlangga, Surabaya, Indonesia

⁵Department of Pharmacy, Faculty of Health Science, University of Darussalam Gontor, Ponorogo, Indonesia

Abstract – Type 2 diabetes mellitus (T2DM) and its complications are important noncommunicable diseases with high mortality rates. Protein tyrosine phosphatase 1B (PTP1B) and aldose reductase inhibitors are recently approached and advanced for T2DM and its complications therapy. *Matricaria chamomilla* L. is acknowledged as a worldwide medicinal herb that has many beneficial health effects as well as antidiabetic effects. Our research was designed to determine the most potential antidiabetic phytochemicals from *M. chamomilla* employing in silico study. 142 phytochemicals were obtained from the databases. The first screening employed iGEMdock and Swiss ADME, involving 93 phytochemicals. Finally, 30 best phytochemicals were docked. Molecular docking and visualization analysis were performed using Avogadro, AutoDock 4.2., and Biovia Discovery Studio 2016. Molecular docking results demonstrate that ligand-protein interaction's binding affinities were -5.16 to -7.54 kcal/mol and -5.30 to -12.10 kcal/mol for PTP1B and aldose reductase protein targets respectively. In silico results demonstrate that *M. chamomilla* has potential antidiabetic phytochemical compounds for T2DM and its complications. We recommended anthecotulide, quercetin, chlorogenic acid, luteolin, and catechin as antidiabetic agents due to their binding affinities against both PTP1B and aldose reductase protein. Those phytochemicals' significant efficacy and potential as antidiabetic must be investigated in further advanced research.

Keywords – *Matricaria chamomilla* L., type 2 diabetes mellitus, in silico, molecular docking, PTP1B, aldose reductase

Introduction

Diabetes mellitus (DM) is one of the most common noncommunicable diseases that burden many countries. The complications lead to a high DM mortality rate.¹ Type 2 DM (T2DM) is the most frequent type of DM commonly caused by insulin resistance due to genetic and environmental factors.² Some pathways induced inflammation, aging, and oxidative stress process catalyzed by several enzymes that lead to insulin response impairment had been distinguished as pathogenesis of T2DM as well as its complications.^{3,4} Research nowadays focused on

finding the best therapeutic protein target to control blood glucose to prevent further complications that lead to mortality.⁵

Protein tyrosine phosphatase 1B (PTP1B) and aldose reductase have been identified as potential protein targets that are recently approached and advanced. Those protein involve in 2 different pathways lead to T2DM progression, morbidity, and complications.⁶ The PTP1B enzyme negatively regulates the insulin signaling process by removing phosphate groups from insulin receptors activated by the insulin receptor substrates (IRS) and blocking signaling molecules like phosphoinositide 3-kinase (PI3K) and protein kinase B (AKT). Furthermore, leptin signaling blocking and endoplasmic reticulum (ER) stress were also initiated by PTP1B. Those pathways lead to insulin resistance, which describes the important role of PTP1B inhibitors in T2DM patients that also had been reported in

*Author for correspondence

Dr. Siti Khaerunnisa, M.Si, Department of Physiology and Medical Biochemistry, Faculty of Medicine, Universitas Airlangga, Mayjen. Prof. Dr. Moestopo St. 47, Surabaya 60132, Indonesia.
Tel: +62-812-3311-8194; E-mail: st.khaerunnisa@fk.unair.ac.id

previous studies.⁷⁻⁹ Aldose reductase is an enzyme that catalyzes the first reaction of the polyol pathway. This reaction produces sorbitol that induces oxidative stress and reduces nicotinamide adenine dinucleotide (NADH), leading to glucose metabolism impairment and diabetic complications.¹⁰ Moreover, aldose reductase inhibitors had been reported as potential antidiabetic agents that prevent and treat diabetic complications.¹¹ Nevertheless, PTP1B and aldose reductase inhibitors drugs have not been approved by Food and Drug Administration (FDA) and some were withdrawn because of their adverse effects and toxicities.⁵

Matricaria chamomilla L. (synonym *Matricaria recutita*) is one of the most popular worldwide medicinal herbs for a long time.¹² Current studies reported many beneficial health effects of *M. chamomilla*, such as sedative and anxiolytic-like effects,¹³ antiproliferative,¹⁴ anticancer,¹⁵ antidiarrheal,¹⁶ antibacterial,¹⁷ antioxidant,¹⁸ and also anti-diabetic. Major bioactive compounds of *M. chamomilla* consist of sesquiterpenic and phenolic compounds. Sesquiterpenic compounds, i.e. alpha-bisabolol, bisabolol oxides A and B, chamazulene, and farnesene, meanwhile apigenin, quercetin, patuletin, coumarin (herniarin and umbelliferon), luteolin and their glucosides, are categorized as phenolic compounds.¹⁹ *M. chamomilla*'s bioactive compounds prevent and treat T2DM and its complication through many mechanisms, such as decreasing the glucose level, increasing insulin sensitivity, inhibiting sorbitol accumulation in erythrocytes, and increasing the antioxidant parameters. Those mechanism could be accomplished by inhibiting PTP1B and aldose reductase protein.²⁰⁻²²

The previous study revealed that in silico methods is capable of predicting drug targets' clinical success.²³ Our in silico study would demonstrate the binding sites of *M. chamomilla*'s bioactive compounds to 2-(oxalyl-amino)-4,5,6,7-tetrahydro-thieno[2,3-c]pyridine-3-carboxylic acid (OTA) and {5-fluoro-2-[(3-nitrobenzyl) carbamoyl]phenoxy} acetic acid (30L) native ligands of PTP1B and aldose reductase protein respectively. Therefore, this study aims to determine the compatibility among the bioactive compounds in *M. chamomilla* with PTP1B and aldose reductase target drugs for T2DM and its complications. The results could be useful for further research, i.e. in vitro and in vivo, and may lead to synthetic compound modification discovery for DM.

Experimental

System Configuration – This research was performed operating Windows 8 Pro OS 64 bit laptop with an Intel

Core i5 processor and 8 GB RAM. iGEMdock, Avogadro, AutoDock 4.2, and Biovia Discovery Studio 2016 were software employed to accomplish the in silico research.

Protein Selection – PTP1B and aldose reductase were protein targets to be inhibited for T2DM therapy. Protein structure of PTP1B and aldose reductase were obtained from RSCB PDB (<https://www.rcsb.org/>) with PDB ID 1C88 and 4QBX. The method of the protein structure determination was X-ray crystallography with X-ray diffraction resolution less than 2.00 Å. Selected 1C88 and 4QBX proteins were visualized in Biovia Discovery Studio 2016 to investigate the native ligand and active site for analyzing the grid box. Biovia Discovery Studio 2016 is a singleunified, easy-to-use, graphical interface for powerful drug design and protein modeling research.²⁴

Phytochemicals Selection – 142 *M. chamomilla* phytochemicals that reported in the previous studies were retrieved from Dr. Duke's Phytochemical and Ethnobotanical database (phytochem.nal.usda.gov/phytochem/search). The 3D structures were obtained from PubChem (pubchem.ncbi.nlm.nih.gov) in .sdf format. The compounds with unavailable structures were excluded. The canonical SMILES were retrieved from PubChem and evaluated by Swiss ADME to examine the drug-likeness based on Lipinski's rule of five. It describes the relationship between the pharmacokinetic and physicochemical parameters.²⁵ The low absorption is predicted if the molecular weight >500, number of hydrogen bond acceptors > 10, number of hydrogen bond donors > 5, and log P (CLogP) > 5.²⁶ 93 phytochemicals were screened by the binding affinity and Lipinski's rule of five obtained from iGEMdock and Swiss ADME respectively. The best 30 phytochemicals from the screening were selected for further docking analysis (Table 1).

Docking and Visualization – Autodock 4.2 was employed for protein preparation. It was performed by removing water and separating it from its native ligand. 1C88 and 4QBX proteins and their (OTA) and (30L) native ligands were optimized by adding polar-only hydrogens, merging nonpolar, adding Kollman charges for proteins, and computing gasteiger for native ligands. Native ligand position on the binding site was determined by arranging the grid box size (XYZ), the center coordinates (X, Y, Z), and the spacing.²⁷ OTA grid was set in 22x34x34 (XYZ) point size, 44.675, 13.647, 2.429 center coordinates, and 0.5 Å spacing. 30L grid was set in 24x30x30 (XYZ) point size, 64.867, -7.141, 37.916 center coordinates, and 0.5 Å spacing.

The phytochemical compounds from *M. chamomilla* would be the ligands that bind to the binding sites of the

Table 1. *M. chamomilla* phytochemical compounds and their ADME analysis

Ligand	CID	Molecular Formula	Lipinski's Rule of 5				TPSA (Å ²)	GI Absorption	
			Molecule weight (≤ 500 g/mol)	H-bond acceptors (n ≤ 10)	H-bond donors (n ≤ 5)	LogP ≤ 5			
6-Methoxykaempferol	5377945	C ₁₆ H ₁₂ O ₇	316.26	7	4	1.6	0	120.36	High
α-Bisabolol	442343	C ₁₅ H ₂₆ O	222.37	1	1	3.76	0	20.23	High
Anthecotulide	11962174	C ₁₅ H ₂₀ O ₃	248.32	3	0	3.01	0	43.37	High
Apigenin	5280443	C ₁₅ H ₁₀ O ₅	270.24	5	3	2.11	0	90.9	High
Apigenin-7-glucoside	5280704	C ₂₁ H ₂₀ O ₁₀	432.38	10	6	0.55	1	170.05	Low
Axillarin	5281603	C ₁₇ H ₁₄ O ₈	346.29	8	4	1.73	0	129.59	High
Azulene	9231	C ₁₀ H ₈	128.17	0	0	3.02	0	0	Low
β-Sitosterol	222284	C ₂₉ H ₅₀ O	414.71	1	1	7.19	1	20.23	Low
Caffeic acid	689043	C ₉ H ₈ O ₄	180.16	4	3	0.93	0	77.76	High
Catechin	9064	C ₁₅ H ₁₄ O ₆	290.27	6	5	0.85	0	110.38	High
Chlorogenic acid	1794427	C ₁₆ H ₁₈ O ₉	354.31	9	6	-0.38	1	164.75	Low
Chrysoeriol	5280666	C ₁₆ H ₁₂ O ₆	300.26	6	3	2.18	0	100.13	High
Chrysosplenetin	5281608	C ₁₉ H ₁₈ O ₈	374.34	8	2	2.49	0	107.59	High
Eupatoletin	5317291	C ₁₇ H ₁₄ O ₈	346.29	8	4	1.72	0	129.59	High
Isoferulic acid	736186	C ₁₀ H ₁₀ O ₄	194.18	4	2	1.39	0	66.76	High
Isorhamnetin	5281654	C ₁₆ H ₁₂ O ₇	316.26	7	4	1.65	0	120.36	High
Jaceidin	5464461	C ₁₈ H ₁₆ O ₈	360.31	8	3	2.15	0	118.59	High
Kaempferol	5280863	C ₁₅ H ₁₀ O ₆	286.24	6	4	1.58	0	111.13	High
Linoleic acid	5280450	C ₁₈ H ₃₂ O ₂	280.45	2	1	5.45	1	37.3	High
Luteolin	5280445	C ₁₅ H ₁₀ O ₆	286.24	6	4	1.73	0	111.13	High
Matricarin	3083923	C ₁₇ H ₂₀ O ₅	304.34	5	0	1.9	0	69.67	High
Oleic acid	445639	C ₁₈ H ₃₄ O ₂	282.46	2	1	5.71	1	37.3	High
Patuletin	5281678	C ₁₆ H ₁₂ O ₈	332.26	8	2	1.38	0	140.59	Low
Quercetagenin-3,6,7,3',4'-pentamethylether	5320351	C ₂₀ H ₂₀ O ₈	388.37	8	1	2.82	0	96.59	High
Quercetin	5280343	C ₁₅ H ₁₀ O ₇	302.24	7	5	1.23	0	131.36	High
Sinapic acid	637775	C ₁₁ H ₁₂ O ₅	224.21	5	2	1.31	0	75.99	High
Spinacetin	5321435	C ₁₇ H ₁₄ O ₈	346.29	8	4	1.8	0	129.59	High
Stigmasterol	5280794	C ₂₉ H ₄₈ O	412.69	1	1	6.96	1	20.23	Low
Thiamine	1130	C ₁₂ H ₁₇ N ₄ OS ⁺	265.35	3	2	0.53	0	104.15	High
Umbeliferone	5281426	C ₉ H ₆ O ₃	162.14	3	1	1.51	0	50.44	High

native ligands. Avogadro and Autodock 4.2 employed ligand preparation. Avogadro performed ligand optimization. Furthermore, ligands optimization were operated by Autodock 4.2, similar to the previous native ligands' process without adding Kollman charges. Ligand positioning based on the binding site of native ligand was saved into .gpf file and the grid would be processed by autogrid4 tools.²⁷

Molecular docking was performed to the ligands under flexible forms interacting with proteins in rigid structures. Ligand tethering to the binding site was accomplished by regulating the genetic algorithms (GA) parameters using 100 GA run and 300 populations. The dock output was

Lamarckian GA and saved in .dpf file that would be processed by autodock4 tools. Finally, the docking analysis and visualization were executed by Autodock 4.2 and Biovia Discovery Studio 2016. The best binding affinity and favorable conformations of the docking results were selected. Furthermore, the binding poses of each ligand with the proteins and their interactions were illustrated.²⁷

Results and Discussion

The most common type of DM is T2DM, which is typically emanated by insulin resistance. T2DM is the

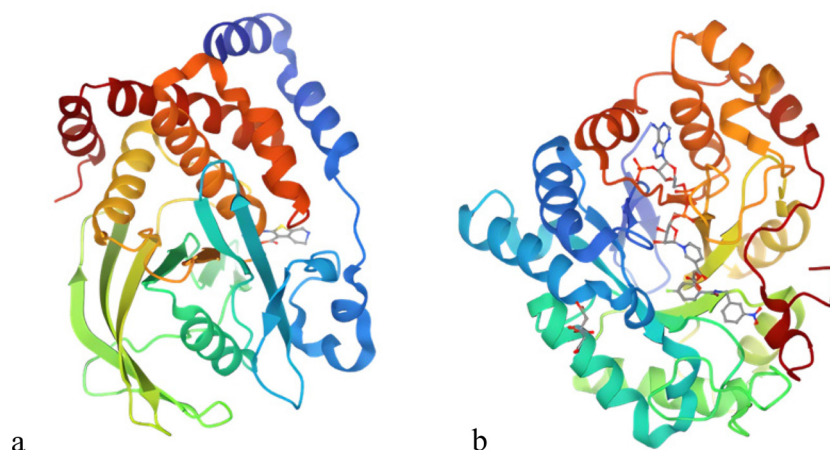


Fig. 1. 3D structure of proteins (a) Protein Tyrosine Phosphatase 1B complexed (1C88), and (b) Aldose Reductase (4QBX).

Table 2. Protein targets, their native ligands, and active sites

Protein Target	PDB ID	Native Ligand	Active Site
OTA			
2-(oxalyl-amino)-4,5,6,7-tetrahydro-thieno[2,3-c]pyridine-3-carboxylic acid			
$C_{10}H_{10}N_2O_5S$			
PTP1B (Protein-Tyrosine Phosphatase 1B) Crystal structure of Protein Tyrosine Phosphatase 1B complexed with 2-(oxalyl-amino)-4,5,6,7-tetrahydro-thieno[2,3-c]pyridine-3-carboxylic acid	1C88		TYR46, ASP48, LYS120, ASP181, PHE182, CYS215, SER216, ALA217, ILE219, GLY 220, ARG221, GLN262, SER285
30L			
{5-fluoro-2-[(3-nitrobenzyl)carbamoyl]phenoxy} acetic acid			
$C_{16}H_{13}FN_2O_6$			
Aldose Reductase Human Aldose Reductase complexed with a ligand with an IDD structure ({5-fluoro-2-(3-nitrobenzyl) carbamoylphenoxy} acetic acid) at 0.98 Å	4QBX		

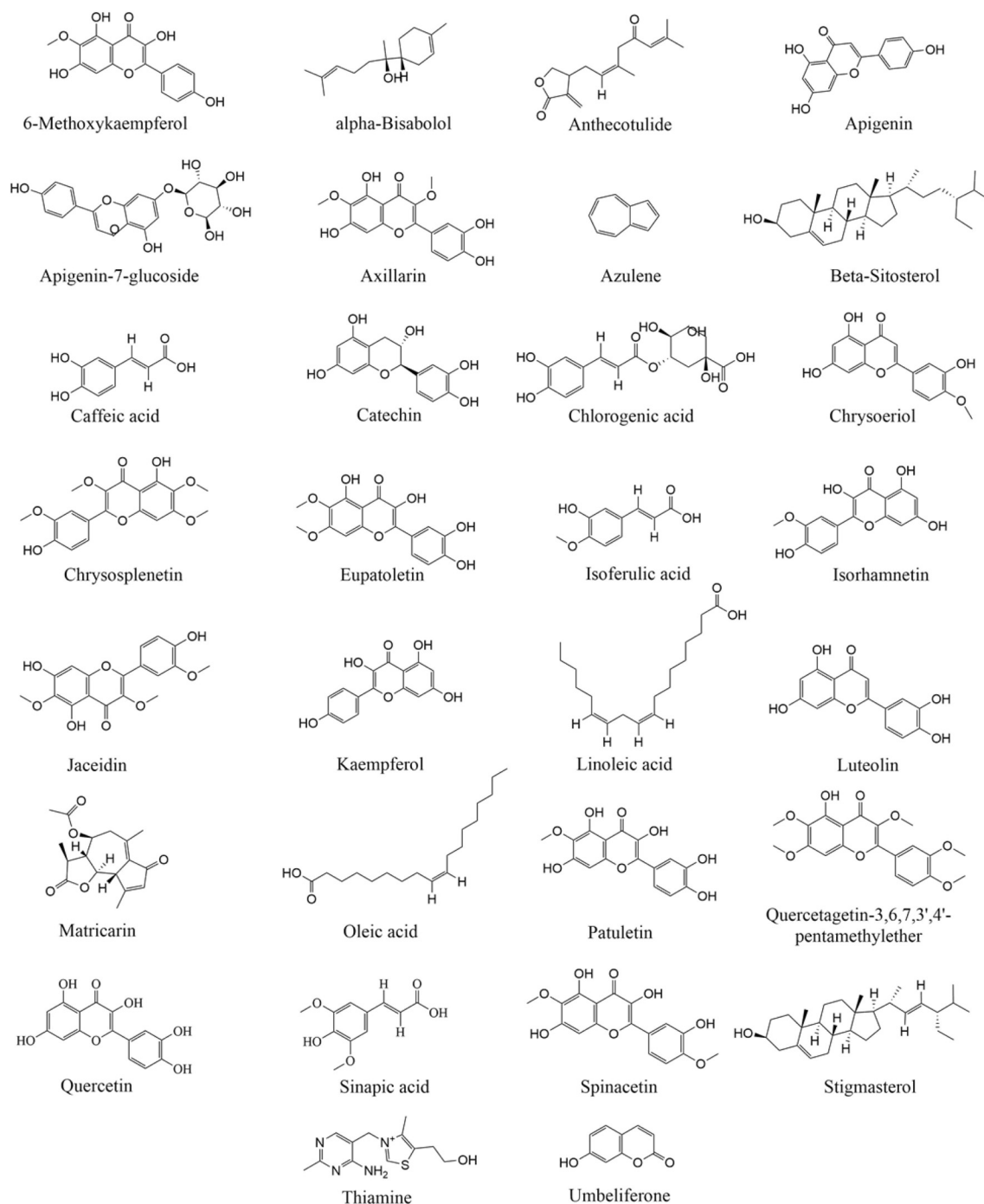


Fig. 2. The structures of *M. chamomilla* phytochemical compounds.

complexed with a ligand with an IDD structure ({5-fluoro-2-[(3-nitrobenzyl)carbamoyl]phenoxy}acetic acid) (Fig. 1b) at 1.80 and 0.98 Å X-ray diffraction resolution respectively. Those proteins have no mutation. Subsequently, OTA and 30L native ligands were separated from their PTP1B and aldose reductase proteins. Table 2 demonstrates the protein targets with their native ligands

and active sites.

Phytochemicals data obtained from PubChem were screened as stated in the experimental. 30 out of 142 phytochemicals were selected for molecular docking (Fig. 2). Due to Lipinski's rule of five, 6 ligands have 1 violation, involving apigenin-7-glucoside and chlorogenic acid with the number of hydrogen donors >5, and β-

sitosterol, linoleic acid, oleic acid, and stigmasterol with $c\text{LogP} > 5$. Apigenin-7-glucoside, azulene, β -sitosterol, chlorogenic acid, patuletin, and stigmasterol have low GI absorption, whereas others have high GI absorption (Table 1).

Table 3 demonstrates the molecular docking analysis of each ligand's most favorable conformations with the

proteins. Lobeglitazone and fidarestat are drugs that act as PTP1B and aldose reductase inhibitors respectively.^{28,29} Most phytochemical ligands have stronger binding affinities than the inhibitory drugs against the protein target. The binding affinity of anthecotulide to 1C88 are the strongest (-7.54 kcal/mol), followed by quercetin, sinapic acid, chlorogenic acid, luteolin, catechin, isoferulic

Table 3. Molecular docking results and visualizations of *M. chamomilla* phytochemicals with the proteins

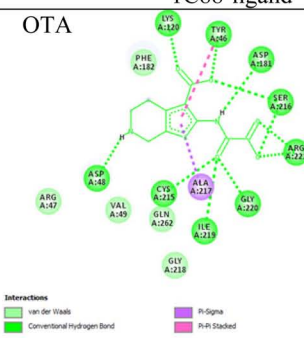
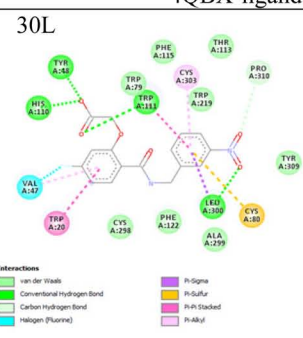

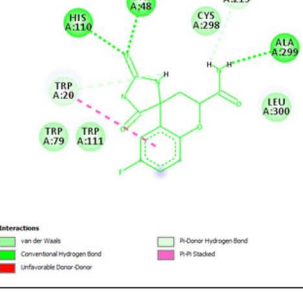
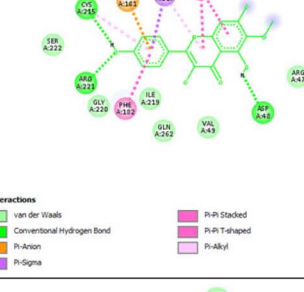
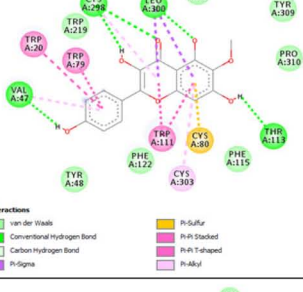
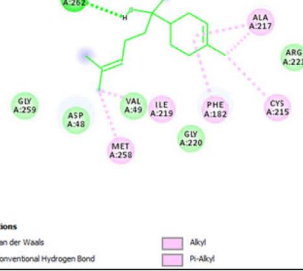
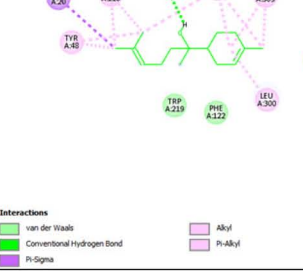
Ligand	1C88-ligand	4QBX-ligand
Native Ligand OTA	 <p>ΔG: -10.14 kcal/mol IC: 36.79 nM Number of H-bond: 12 Number of Hydrophobic bond: 2</p>	 <p>ΔG: -8.97 kcal/mol IC: 263.88 nM Number of H-bond: 6 Number of Hydrophobic bond: 7</p>
Inhibitory Drugs Lobeglitazone	 <p>ΔG: -6.12 kcal/mol IC: 32.54 μM Number of H-bond: 5 Number of Hydrophobic bond: 2</p>	 <p>ΔG: -7.35 kcal/mol IC: 4.12 μM Number of H-bond: 4 Number of Hydrophobic bond: 1</p>
6-Methoxy kaempferol	 <p>ΔG: -6.5 kcal/mol IC: 17.12 μM Number of H-bond: 3 Number of Hydrophobic bond: 6</p>	 <p>ΔG: -8.97 kcal/mol IC: 263.88 nM Number of H-bond: 6 Number of Hydrophobic bond: 12</p>
α -bisabolol	 <p>ΔG: -6.04 kcal/mol IC: 37.64 μM Number of H-bond: 1 Number of Hydrophobic bond: 5</p>	 <p>ΔG: -8.37 kcal/mol IC: 730.9 nM Number of H-bond: 1 Number of Hydrophobic bond: 14</p>

Table 3. continued

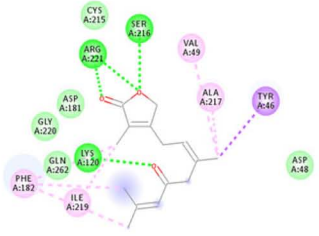
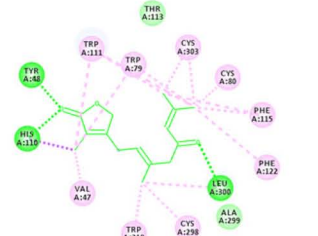
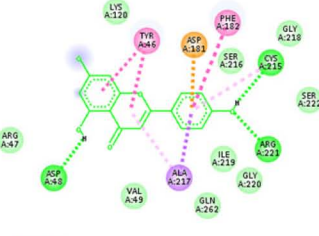
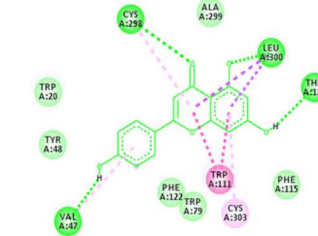
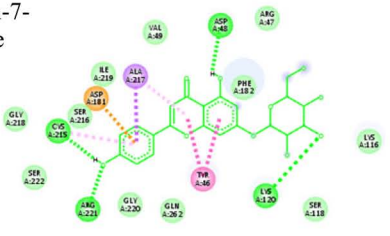
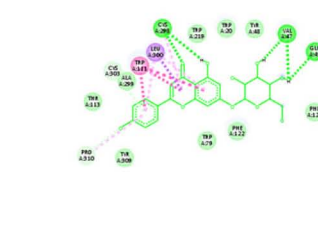
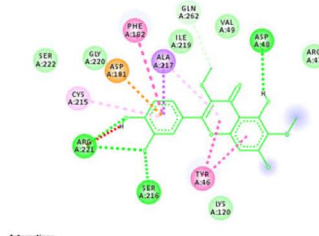
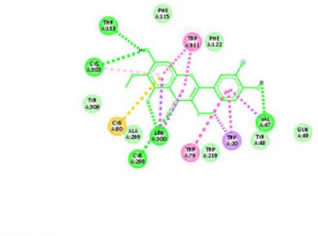
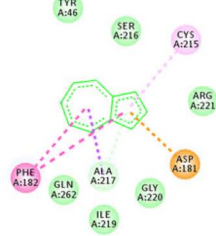
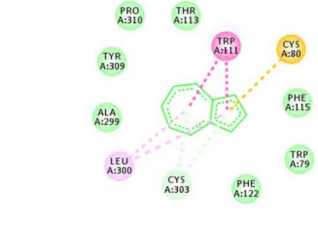
<p>Anthecotulide</p>  <p>Interactions</p> <ul style="list-style-type: none"> van der Waals Conventional Hydrogen Bond Pi-Sigma Alkyl Pi-Alkyl 	<p>ΔG: -7.54 kcal/mol</p> <p>IC: 2.99 μM</p> <p>Number of H-bond: 5</p> <p>Number of Hydrophobic bond: 7</p>	 <p>Interactions</p> <ul style="list-style-type: none"> van der Waals Conventional Hydrogen Bond Pi-Sigma Alkyl Pi-Alkyl 	<p>ΔG: -9.85 kcal/mol</p> <p>IC: 60.54 nM</p> <p>Number of H-bond: 3</p> <p>Number of Hydrophobic bond: 16</p>
<p>Apigenin</p>  <p>Interactions</p> <ul style="list-style-type: none"> van der Waals Conventional Hydrogen Bond Pi-Anion Pi-Sigma Pi-Pi Stacked Pi-Pi T-shaped Pi-Alkyl 	<p>ΔG: -6.98 kcal/mol</p> <p>IC: 7.6 μM</p> <p>Number of H-bond: 3</p> <p>Number of Hydrophobic bond: 6</p>	 <p>Interactions</p> <ul style="list-style-type: none"> van der Waals Conventional Hydrogen Bond Carbon Hydrogen Bond Pi-Sigma Pi-Pi Stacked Pi-Alkyl 	<p>ΔG: -8.81 kcal/mol</p> <p>IC: 347.7 nM</p> <p>Number of H-bond: 5</p> <p>Number of Hydrophobic bond: 9</p>
<p>Apigenin-7-glucoside</p>  <p>Interactions</p> <ul style="list-style-type: none"> van der Waals Conventional Hydrogen Bond Pi-Anion Pi-Sigma Pi-Pi Stacked Pi-Alkyl 	<p>ΔG: -6.52 kcal/mol</p> <p>IC: 16.49 μM</p> <p>Number of H-bond: 4</p> <p>Number of Hydrophobic bond: 5</p>	 <p>Interactions</p> <ul style="list-style-type: none"> van der Waals Conventional Hydrogen Bond Carbon Hydrogen Bond Pi-Donor Hydrogen Bond Pi-Sigma Pi-Pi Stacked Pi-Alkyl 	<p>ΔG: -8.61 kcal/mol</p> <p>IC: 491.55 nM</p> <p>Number of H-bond: 7</p> <p>Number of Hydrophobic bond: 11</p>
<p>Axillarlin</p>  <p>Interactions</p> <ul style="list-style-type: none"> van der Waals Conventional Hydrogen Bond Carbon Hydrogen Bond Unfavorable Donor-Donor Pi-Anion Pi-Sigma Pi-Pi Stacked Pi-Pi T-shaped Pi-Alkyl 	<p>ΔG: -6.74 kcal/mol</p> <p>IC: 11.42 μM</p> <p>Number of H-bond: 5</p> <p>Number of Hydrophobic bond: 6</p>	 <p>Interactions</p> <ul style="list-style-type: none"> van der Waals Conventional Hydrogen Bond Carbon Hydrogen Bond Pi-Donor Hydrogen Bond Pi-Sigma Pi-Pi Stacked Pi-Pi T-shaped Pi-Alkyl Pi-Sulfur 	<p>ΔG: - 8.96 kcal/mol</p> <p>IC: 268.61 nM</p> <p>Number of H-bond: 5</p> <p>Number of Hydrophobic bond: 13</p>
<p>Azulene</p>  <p>Interactions</p> <ul style="list-style-type: none"> van der Waals Pi-Anion Pi-Donor Hydrogen Bond Pi-Sigma Pi-Pi T-shaped Pi-Alkyl 	<p>ΔG: -5.45 kcal/mol</p> <p>IC: 100.8 μM</p> <p>Number of H-bond: 1</p> <p>Number of Hydrophobic bond: 5</p>	 <p>Interactions</p> <ul style="list-style-type: none"> van der Waals Pi-Donor Hydrogen Bond Pi-Pi Stacked Pi-Alkyl Pi-Sulfur 	<p>ΔG: -6.97 kcal/mol</p> <p>IC: 7.82 μM</p> <p>Number of H-bond: 2</p> <p>Number of Hydrophobic bond: 6</p>

Table 3. continued

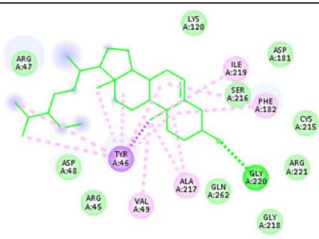
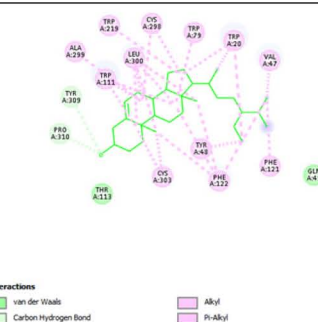
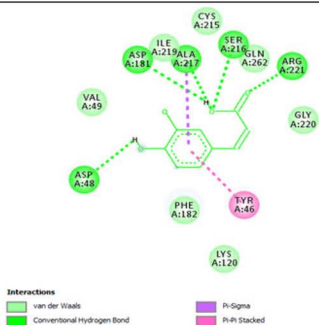
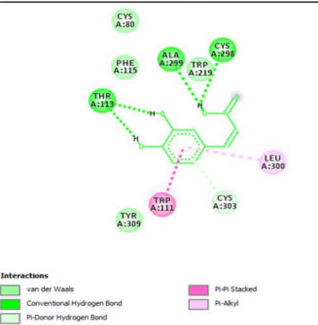
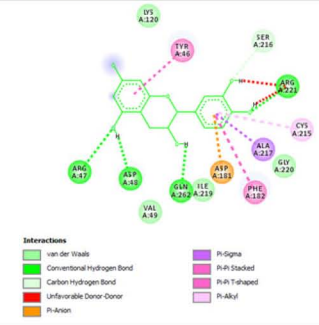
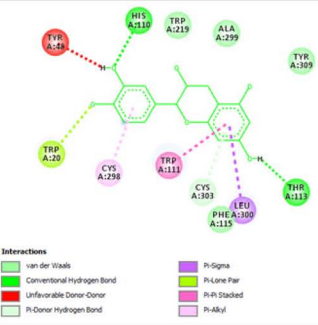
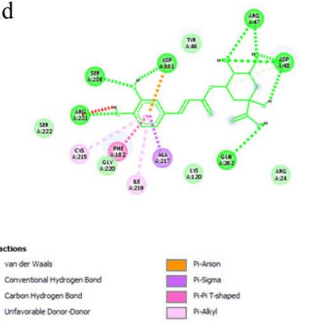
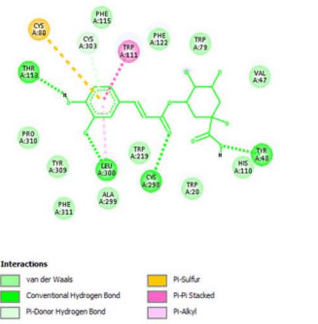
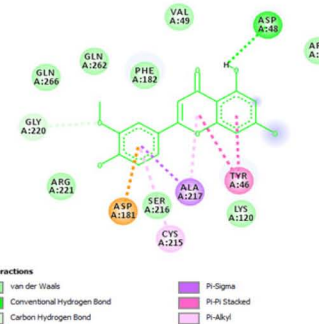
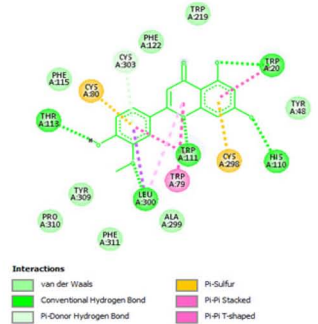
β-sitosterol		ΔG : -6.03 kcal/mol IC: 38.29 μM Number of H-bond: 1 Number of Hydrophobic bond: 7		ΔG : -11.81 kcal/mol IC: 2.21 nM Number of H-bond: 2 Number of Hydrophobic bond: 29
Caffeic Acid		ΔG : -6.63 kcal/mol IC: 13.78 μM Number of H-bond: 6 Number of Hydrophobic bond: 2		ΔG : -5.3 kcal/mol IC: 129.26 μM Number of H-bond: 5 Number of Hydrophobic bond: 3
Catechin		ΔG : -7.07 kcal/mol IC: 6.61 μM Number of H-bond: 5 Number of Hydrophobic bond: 4		ΔG : -8.49 kcal/mol IC: 602.76 nM Number of H-bond: 3 Number of Hydrophobic bond: 4
Chlorogenic acid		ΔG : -7.11 kcal/mol IC: 6.19 μM Number of H-bond: 13 Number of Hydrophobic bond: 4		ΔG : -7.87 kcal/mol IC: 1.69 μM Number of H-bond: 6 Number of Hydrophobic bond: 3
Chrysoeriol		ΔG : -6.96 kcal/mol IC: 7.91 μM Number of H-bond: 2 Number of Hydrophobic bond: 5		ΔG : -9.49 kcal/mol IC: 110.87 nM Number of H-bond: 6 Number of Hydrophobic bond: 7

Table 3. continued

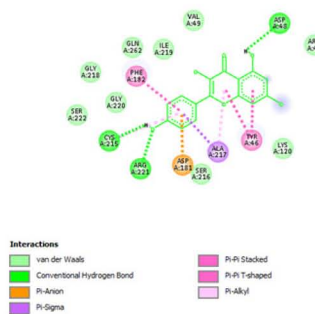
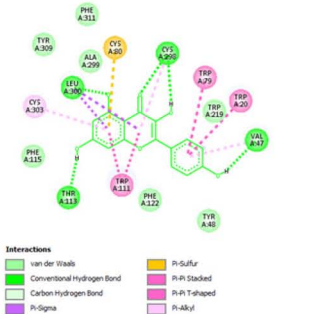
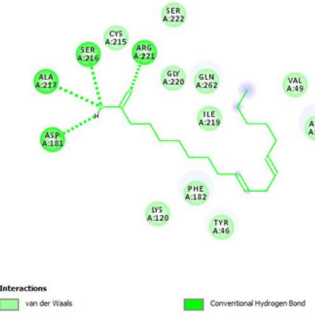
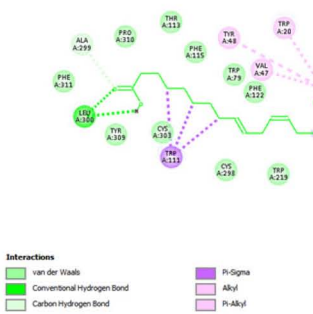
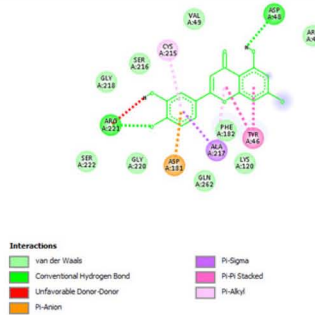
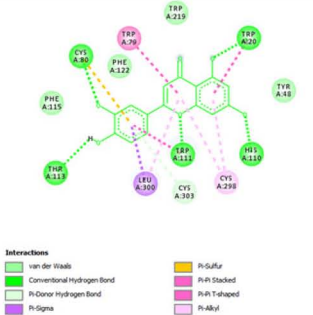
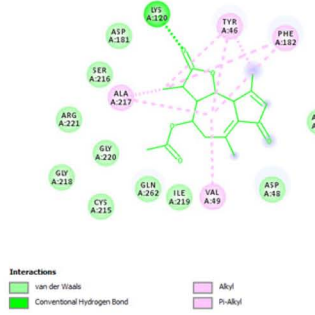
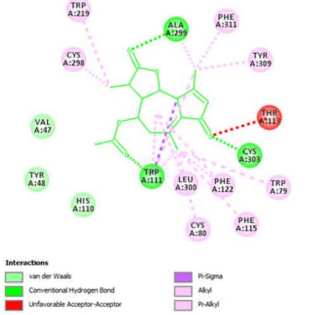
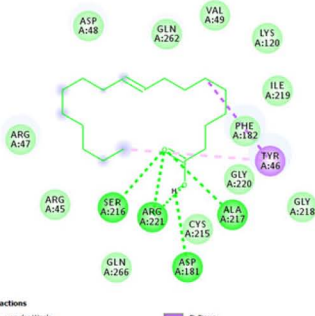
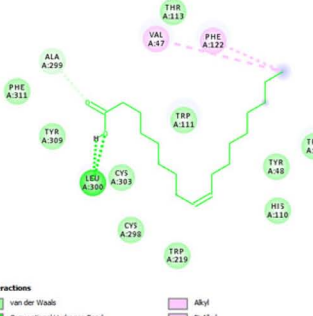
Kaempferol	 <p>Interactions</p> <ul style="list-style-type: none"> van der Waals Conventional Hydrogen Bond Pi-Anion Pi-Sigma Pi-Pi Stacked Pi-Pi T-shaped Pi-Alkyl 	ΔG : -6.7 kcal/mol IC: 12.27 μM Number of H-bond: 3 Number of Hydrophobic bond: 6	 <p>Interactions</p> <ul style="list-style-type: none"> van der Waals Conventional Hydrogen Bond Carbon Hydrogen Bond Pi-Sulfur Pi-Pi Stacked Pi-Pi T-shaped Pi-Alkyl 	ΔG : -8.57 kcal/mol IC: 519.74 nM Number of H-bond: 6 Number of Hydrophobic bond: 12
Linoleic Acid	 <p>Interactions</p> <ul style="list-style-type: none"> van der Waals Conventional Hydrogen Bond 	ΔG : -5.66 kcal/mol IC: 71.18 μM Number of H-bond: 5 Number of Hydrophobic bond: 0	 <p>Interactions</p> <ul style="list-style-type: none"> van der Waals Conventional Hydrogen Bond Carbon Hydrogen Bond Pi-Sigma Alkyl Pi-Alkyl 	ΔG : -6.67 kcal/mol IC: 12.9 μM Number of H-bond: 3 Number of Hydrophobic bond: 7
Luteolin	 <p>Interactions</p> <ul style="list-style-type: none"> van der Waals Conventional Hydrogen Bond Unfavorable Donor-Donor Pi-Sigma Pi-Pi Stacked Pi-Alkyl 	ΔG : -7.1 kcal/mol IC: 6.23 μM Number of H-bond: 2 Number of Hydrophobic bond: 5	 <p>Interactions</p> <ul style="list-style-type: none"> van der Waals Conventional Hydrogen Bond Pi-Donor Hydrogen Bond Pi-Sigma Pi-Sulfur Pi-Pi Stacked Pi-Pi T-shaped Pi-Alkyl 	ΔG : -8.63 kcal/mol IC: 471.13 nM Number of H-bond: 6 Number of Hydrophobic bond: 9
Matricarin	 <p>Interactions</p> <ul style="list-style-type: none"> van der Waals Conventional Hydrogen Bond Alkyl Pi-Alkyl 	ΔG : -5.88 kcal/mol IC: 49.35 μM Number of H-bond: 1 Number of Hydrophobic bond: 8	 <p>Interactions</p> <ul style="list-style-type: none"> van der Waals Conventional Hydrogen Bond Unfavorable Acceptor-Acceptor Pi-Sigma Alkyl Pi-Alkyl 	ΔG : -8.82 kcal/mol IC: 340.52 nM Number of H-bond: 3 Number of Hydrophobic bond: 16
Oleic acid	 <p>Interactions</p> <ul style="list-style-type: none"> van der Waals Conventional Hydrogen Bond Pi-Sigma Pi-Alkyl 	ΔG : -5.16 kcal/mol IC: 165.75 μM Number of H-bond: 6 Number of Hydrophobic bond: 2	 <p>Interactions</p> <ul style="list-style-type: none"> van der Waals Conventional Hydrogen Bond Carbon Hydrogen Bond Alkyl Pi-Alkyl 	ΔG : -6.44 kcal/mol IC: 19.1 μM Number of H-bond: 3 Number of Hydrophobic bond: 2

Table 3. continued

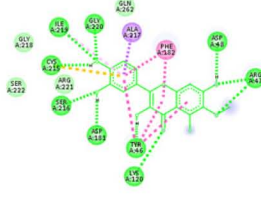
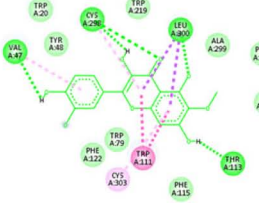
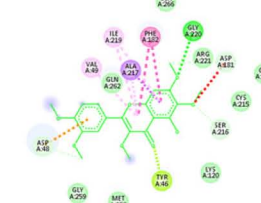
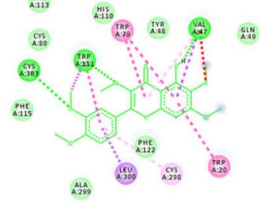
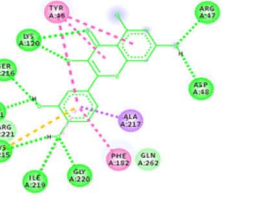
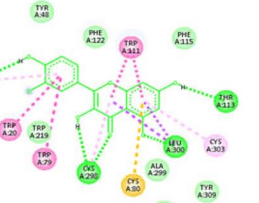
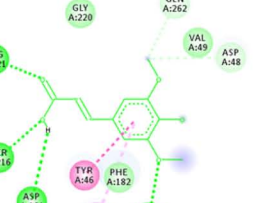
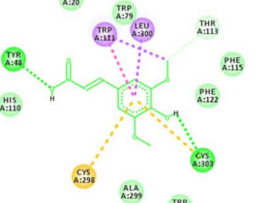

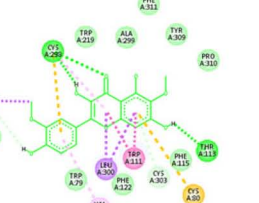
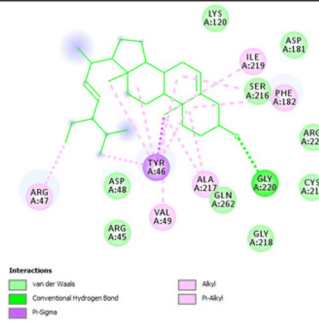
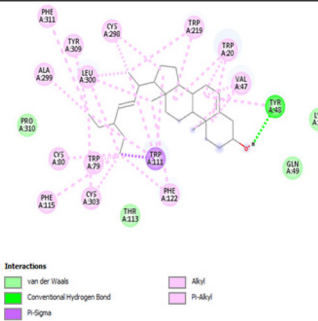
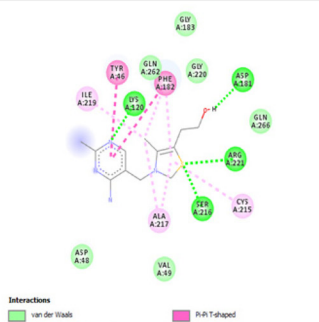
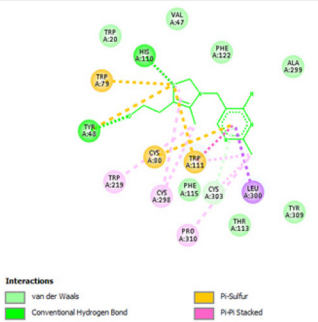
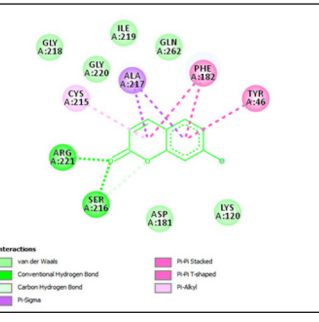
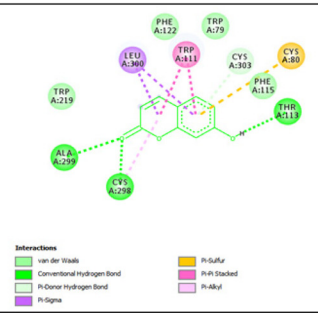
<p>Patuletin</p>  <p>Interactions</p> <ul style="list-style-type: none"> van der Waals Conventional Hydrogen Bond Pi-Sigma Pi-Sulfur Pi-Pi Stacked Pi-Pi T-shaped Pi-Alkyl 	<p>ΔG: -6.87 kcal/mol</p> <p>IC: 9.15 μM</p> <p>Number of H-bond: 10</p> <p>Number of Hydrophobic bond: 7</p>	 <p>Interactions</p> <ul style="list-style-type: none"> van der Waals Conventional Hydrogen Bond Carbon Hydrogen Bond Pi-Sigma Pi-Pi Stacked Pi-Alkyl 	<p>ΔG: -8.65 kcal/mol</p> <p>IC: 456.68 nM</p> <p>Number of H-bond: 6</p> <p>Number of Hydrophobic bond: 9</p>
<p>Quercetagetin-3,6,7,3',4'-pentamethylether</p>  <p>Interactions</p> <ul style="list-style-type: none"> van der Waals Conventional Hydrogen Bond Carbon Hydrogen Bond Unfavorable Acceptor-Acceptor Pi-Sulfur Pi-Sigma Pi-Lone Pair Pi-Pi T-shaped Pi-Alkyl 	<p>ΔG: -6.52 kcal/mol</p> <p>IC: 16.73 μM</p> <p>Number of H-bond: 4</p> <p>Number of Hydrophobic bond: 7</p>	 <p>Interactions</p> <ul style="list-style-type: none"> van der Waals Conventional Hydrogen Bond Unfavorable Acceptor-Acceptor Pi-Sigma Pi-Pi Stacked Pi-Pi T-shaped Pi-Alkyl 	<p>ΔG: -9.66 kcal/mol</p> <p>IC: 82.99 nM</p> <p>Number of H-bond: 4</p> <p>Number of Hydrophobic bond: 10</p>
<p>Quercetin</p>  <p>Interactions</p> <ul style="list-style-type: none"> van der Waals Conventional Hydrogen Bond Carbon Hydrogen Bond Pi-Sigma Pi-Sulfur Pi-Pi Stacked Pi-Pi T-shaped Pi-Alkyl 	<p>ΔG: -7.31 kcal/mol</p> <p>IC: 4.41 μM</p> <p>Number of H-bond: 6</p> <p>Number of Hydrophobic bond: 6</p>	 <p>Interactions</p> <ul style="list-style-type: none"> van der Waals Conventional Hydrogen Bond Carbon Hydrogen Bond Pi-Sigma Pi-Sulfur Pi-Pi Stacked Pi-Pi T-shaped Pi-Alkyl 	<p>ΔG: -8.25 kcal/mol</p> <p>IC: 903.97 nM</p> <p>Number of H-bond: 6</p> <p>Number of Hydrophobic bond: 12</p>
<p>Sinapic acid</p>  <p>Interactions</p> <ul style="list-style-type: none"> van der Waals Conventional Hydrogen Bond Carbon Hydrogen Bond Pi-Sigma Pi-Sulfur Pi-Pi Stacked Pi-Alkyl 	<p>ΔG: -7.12 kcal/mol</p> <p>IC: 6.06 μM</p> <p>Number of H-bond: 6</p> <p>Number of Hydrophobic bond: 2</p>	 <p>Interactions</p> <ul style="list-style-type: none"> van der Waals Conventional Hydrogen Bond Carbon Hydrogen Bond Pi-Sigma Pi-Sulfur Pi-Pi Stacked Pi-Alkyl 	<p>ΔG: -5.84 kcal/mol</p> <p>IC: 52.02 μM</p> <p>Number of H-bond:</p> <p>Number of Hydrophobic bond: 5</p>
<p>Spinacetin</p>  <p>Interactions</p> <ul style="list-style-type: none"> van der Waals Conventional Hydrogen Bond Carbon Hydrogen Bond Unfavorable Donor-Donor Pi-Arson Pi-Sigma Pi-Pi Stacked Pi-Alkyl 	<p>ΔG: -6.39 kcal/mol</p> <p>IC: 20.73 μM</p> <p>Number of H-bond: 4</p> <p>Number of Hydrophobic bond: 5</p>	 <p>Interactions</p> <ul style="list-style-type: none"> van der Waals Conventional Hydrogen Bond Carbon Hydrogen Bond Pi-Donor Hydrogen Bond Pi-Sigma Pi-Sulfur Pi-Pi Stacked Pi-Alkyl 	<p>ΔG: -9.18 kcal/mol</p> <p>IC: 187.7 nM</p> <p>Number of H-bond: 5</p> <p>Number of Hydrophobic bond: 9</p>

Table 3. continued

Stigmasterol	 <p> ΔG: -6.3 kcal/mol IC: 24.12 μM Number of H-bond: 1 Number of Hydrophobic bond: 13 </p>	 <p> ΔG: -12.1 kcal/mol IC: 1.35 nM Number of H-bond: 1 Number of Hydrophobic bond: 35 </p>
Thiamine	 <p> ΔG: -6.26 kcal/mol IC: 24.14 μM Number of H-bond: 4 Number of Hydrophobic bond: 8 </p>	 <p> ΔG: -7.9 kcal/mol IC: 1.63 μM Number of H-bond: Number of Hydrophobic bond: 11 </p>
Umbeliferone	 <p> ΔG: -6.51 kcal/mol IC: 16.77 μM Number of H-bond: 4 Number of Hydrophobic bond: 6 </p>	 <p> ΔG: -6.98 kcal/mol IC: 7.66 μM Number of H-bond: 4 Number of Hydrophobic bond: 7 </p>

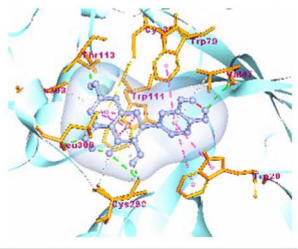
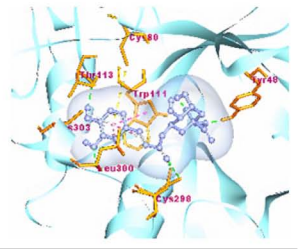
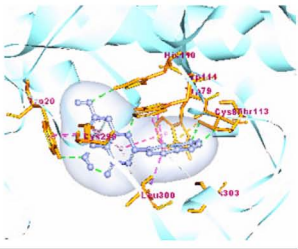
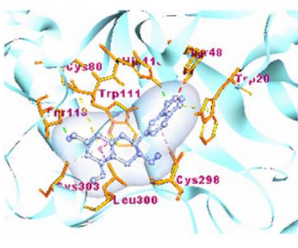
acid, apigenin, chrysoeriol, patuletin, eupatoletin, axillarin, kaempferol, caffeic acid, isorhamnetin, apigenin-7-glucoside, quercetagenin-3,6,7,3',4'-pentamethylether, umbelliferone, 6-methoxykaempferol, jaceidin, chrysopenetin, spinacetin, stigmasterol, and thiamine (-7.31 to -6.26 kcal/mol) that have more negative binding affinity than lobeglitazone (-6.12 kcal/mol). On the other hand, the binding affinity between stigmasterol and 4QBX protein targets are the strongest (-12.1 kcal/mol), followed by β -sitosterol, anthecotulide, quercetagenin-3,6,7,3',4'-pentamethylether, chrysoeriol, jaceidin, spinacetin, 6-methoxykaempferol, axillarin, chrysopenetin, matricarin, isorhamnetin, apigenin, patuletin, luteolin, apigenin-7-glucoside, kaempferol, catechin, α -bisabolol, quercetin, eupatoletin, thiamine, and chlorogenic acid (-11.81 to -7.87 kcal/mol) that have more negative binding affinity than fidarestat (-7.35 kcal/mol).

Generally, binding affinities and inhibitory constants in ligands-4QBX protein interactions are better than ligands-1C88 protein interactions. Stigmasterol and β -sitosterol have the strongest binding affinities and more negative binding affinities than the native ligand against 4QBX protein. Moreover, the inhibitory constants are relatively low. It describes their great potential to inhibit aldose reductase. Contrary to ligands-4QBX protein interaction, those phytosterol compounds have much weaker binding affinity than the others against 1C88. Furthermore, those phytosterol compounds predominate in human dietary nutrition and had important roles in organism physiology.³⁰ An improvement in glycemic control by activating the insulin receptor and GLUT 4 was demonstrated after both phytochemicals were given orally.^{31,32} Moreover, Reza et al.³³ revealed antidiabetic effects of stigmasterol and β -sitosterol by inhibiting DPP-4 and α -glucosidase respec-

Table 4. Molecular docking results and visualization of five best phytochemicals

Protein	Ligand	H-Bond (Å)	Hydrophobic Interaction (Å)	3D Visualization
1C88	Anthecotulide	LYS120 (1.81), SER216 (2.36), ARG221 (1.62; 1.98; 2.01)	TYR46 (3.69), VAL49 (4.65), PHE182 (4.49; 4.57; 5.29), ALA217 (3.95), ILE219 (5.31)	
	Quercetin	ARG47 (2.03), ASP48 (1.85), LYS120 (1.73; 2.64), ASP181 (1.76), CYS215 (2.58), SER216 (2.72; 3.26), ILE219 (2.68), GLY220 (1.92)	TYR46 (4.05; 5.24; 5.38), PHE182 (4.61), ALA217 (3.11), ILE219 (5.49)	
	Chlorogenic acid	ARG47 (1.98; 3.02; 3.09), ASP48 (1.70; 2.05, 2.41; 3.29; 3.50), ASP181 (2.03), SER216 (2.38; 3.02), ARG221 (1.97), GLN262 (2.61)	PHE182 (4.52), CYS215 (5.32), ALA217 (3.47), ILE219 (5.43)	
	Luteolin	ASP48 (2.01), ARG221 (1.81)	TYR46 (3.68; 3.78), CYS215 (4.35), ALA217 (3.77; 4.35)	
	Catechin	ARG47 (2.92), ASP48 (1.92), SER216 (2.79), ARG221 (2.01), GLN262 (1.97)	TYR46 (4.27), PHE182 (4.52), CYS215 (5.15), ALA217 (3.60)	
4QBX	Anthecotulide	TYR48 (1.95), HIS110 (1.87), LEU300 (2.57)	VAL47 (4.16), TRP79 (4.26;4.44), CYS80 (4.11), HIS110 (3.62), TRP111 (4.05;4.06; 4.23), PHE115 (4.33; 5.39), PHE122 (4.43), TRP219 (4.16), CYS298 (4.23), LEU300 (3.80), CYS303 (3.84; 4.94)	

Table 4. continued

Quercetin	VAL47 (2.90), THR113 (1.98), CYS298 (2.57; 3.41; 3.47), LEU300 (2.35)	TRP20 (4.99; 5.40), VAL47 (4.54), TRP79 (5.31), TRP111 (3.56; 3.76; 4.10; 4.15), CYS298 (5.31), LEU300 (3.73; 3.76), CYS303 (4.63)	
Chlorogenic acid	TYR48 (1.75), THR113 (2.19), CYS298 (2.87; 3.40), LEU300 (2.53), CYS303 (3.79)	TRP111 (3.62; 4.10), LEU300 (4.59)	
Luteolin	TRP20 (2.65), CYS80 (3.25), HIS110 (2.51), TRP111 (2.30), THR113 (2.29), CYS303 (4.11)	TRP20 (4.51; 4.63), TRP79 (5.64), TRP111 (3.61; 3.79), CYS298 (5.40; 5.45); LEU300 (3.82; 5.37)	
Catechin	HIS110 (2.25), THR113 (1.87), CYS303 (3.72)	TRP111 (3.74; 4.20), CYS298 (5.19), LEU300 (3.88)	

tively. Nevertheless, antioxidant, anti-inflammatory, immunomodulatory, and antilipidemic effects of phytosterol related to T2DM and its complications were established as well.³⁴ On the other hand, phenolic acid i.e. sinapic acid, chlorogenic acid, isoferulic acid, and caffeic acid,³⁵ have relatively strong binding affinities against 1C88. Contrary to ligands-1C88 interactions, binding affinities between those phenolic acids and 4QBX are relatively weaker than the others, except for chlorogenic acid. Related to that, phenolic acids were proven to prevent the inactivation of the PI3K-AKT pathway, similar to PTP1B inhibitor's mechanism of action.^{7,36}

Molecular docking results establish that all of the ligands successfully bind to the proteins' active sites. The interactions between ligands and amino acids are visualized in 2D diagrams (Table 3), which described that

all *M. chamomilla* phytochemical compounds that we docked could provide strong and stable complexes with both 1C88 and 4QBX. Nevertheless, the stability of ligand-protein interaction is determined by the magnitude of negative binding affinity. Hydrophobic interaction and hydrogen bond contribute to maintaining the protein structure and stability as well as lowering the binding affinity of the protein-ligand complex. Therefore, the amount of hydrophobic interaction and hydrogen bond play important role as well.^{37,38} As the results, anthecotulide, quercetin, chlorogenic acid, luteolin, and catechin are ligands that have the best five ligand-protein interactions both to 1C88 and 4QBX proteins that were visualized in 3D diagrams. Furthermore, the results also describe the amino acids involved in each variety of interaction and the distances(Å) (Table 4).

Anthecotulide has the first and third strongest binding affinity against 1C88 and 4QBX respectively. Additionally, anthecotulide has sesquiterpene lactones (SLs) structure that is well known to have antidiabetic effects that increase insulin sensitivity,^{22, 39-40} in accordance with our results. Moreover, phenolic compounds i.e. quercetin, chlorogenic acid, luteolin, and catechin also have great binding affinities against both 1C88 and 4QBX. Bule et al.⁴¹ and Jaishree et al.⁴² reported that quercetin had antidiabetic effects as well as reduce the risk of T2DM. Quercetin was proven to lower blood glucose through inhibiting α -glucosidase in vitro and promoting insulin action by improving skeletal muscle mitochondrial biogenesis.⁴¹ Peripheral neuropathy, as one of the main complications of T2DM, was reported to be improved by quercetin consumption.⁴³ Chlorogenic acid was reported to have glucose and lipid metabolism regulation effects.³⁶ Ali et al.⁴⁴ reported that luteolin and its derivatives act as non-competitive inhibitors of PTP1B. Furthermore, luteolin protected the cardiac tissues against diabetic cardiomyopathy as one of diabetic complications.⁴⁵ Luteolin also contributed to protecting the liver and renal function by reducing uric acid levels in liver tissue and hyperuricemia mice.^{46,47} Catechin could ameliorate diabetic autonomic nephropathy, provide antibacterial effect, and enhance intestinal immunity.^{48,49} Those phenolic compounds were described to have antioxidant effects that antagonize reactive oxygen species (ROS) along with the inflammation, which is believed to be the underlying pathology of T2DM and its complications.^{42,50,51} Finally, these five best phytochemicals have the potential to be oral antidiabetic drug compounds due to their drug-likeness based on Lipinski's rule of five.

In conclusion, the in silico molecular docking results demonstrate that *M. chamomilla* has potential antidiabetic phytochemical compounds for T2DM and its complications. Anthecotulide, quercetin, chlorogenic acid, luteolin, and catechin are the most recommended antidiabetic agents due to their binding affinities against both PTP1B and aldose reductase protein. Finally, the significant efficacy and potential of the compounds above as antidiabetic agents must be investigated by further researches such as in vitro, in vivo, and also clinical trials in advance.

Acknowledgments

The authors would like to thank the Dean of Faculty of Medicine, Universitas Airlangga, who kindly support this in silico study.

References

- (1) International Diabetes Federation. IDF DIABETES ATLAS vol. 8th Edition; Karuranga, S.; Fernandes, J. R.; Huang, Y.; Malanda, B. Ed; International Diabetes Federation; Belgium, **2017**, pp 14-95.
- (2) American Diabetes Association. Diabetes Care: Standards of Medical Care in Diabetes; Riddle, M. C. Ed; USA, **2019**, pp S13-S28.
- (3) Halim, M.; Halim, A. *Diabetes Metab. Syndr.* **2019**, *13*, 1165-1172.
- (4) Brownlee, M. *Diabetes* **2005**, *54*, 1615-1625.
- (5) Dowarah, J.; Singh, V. P. *Bioorg. Med. Chem.* **2020**, *28*, 115263.
- (6) Artasensi, A.; Pedretti, A.; Vistoli, G.; Fumagalli, L. *Molecules* **2020**, *25*, 1987.
- (7) Qian, S.; Zhang, M.; He, Y.; Wang, W.; Liu, S. *Future Med. Chem.* **2016**, *8*, 1239-1258.
- (8) Hussain, H.; Green, I. R.; Abbas, G.; Adekenov, S. M.; Hussain, W.; Ali, I. *Expert Opin. Ther. Pat.* **2019**, *29*, 689-702.
- (9) Verma, M.; Gupta, S. J.; Chaudhary, A.; Garg, V. K. *Bioorg. Chem.* **2017**, *70*, 267-283.
- (10) Yan, L. *J. Animal Model Exp. Med.* **2018**, *1*, 7-13.
- (11) Grewal, A. S.; Bhardwaj, S.; Pandita, D.; Lather, V.; Sekhon, B. S. *Mini Rev. Med. Chem.* **2016**, *16*, 120-162.
- (12) Singh, O.; Khanam, Z.; Misra, N.; Srivastava, M. K. *Pharmacogn. Rev.* **2011**, *5*, 82-95.
- (13) Chaves, P. F. P.; Hocayen, P.A.S.; Dallazen, J. L.; de Paula Werner, M. F.; Iacomini, M.; Andreatini, R.; Cordeiro, L. M. C. *Int. J. Biol. Macromol.* **2020**, *164*, 1675-1682.
- (14) Ubessi, C.; Tedesco, S. B.; de Bona da Silva, C.; Baldoni, M.; Kryszczun, D. K.; Heinzmann, B. M.; Rosa, I. A.; Mori, N. C. *J. Ethnopharmacol.* **2019**, *239*, 111907.
- (15) Al-Dabbagh, B.; Elhaty, I. A.; Elhaw, M.; Murali, C.; Al-Mansoori, A.; Awad, B.; Amin, A. *BMC Res. Notes* **2019**, *12*, 1-8.
- (16) Díaz, A.; Vargas-Perez, I.; Aguilar-Cruz, L.; Calva-Rodríguez, R.; Treviño, S.; Venegas, B.; Contreras-Mora, I. R. *Rev. Bras. Farmacogn.* **2014**, *24*, 419-424.
- (17) Parlinska-Wojtan, M.; Kus-Liskiewicz, M.; Depciuch, J.; Sadik, O. *Bioprocess Biosyst. Eng.* **2016**, *39*, 1213-1223.
- (18) Agatonovic-Kustrin, S.; Babazadeh-Ortakand, D.; Morton, D. W.; Yusof, A. P. *J. Chromatogr. A.* **2015**, *1385*, 103-110.
- (19) Petronilho, S.; Maraschin, M.; Coimbra, M. A.; Rocha, S. M. *Ind. Crops Prod.* **2012**, *40*, 1-12.
- (20) Zemestani, M.; Rafraf, M.; Asghari-Jafarabadi, M. *Nutrition* **2016**, *32*, 66-72.
- (21) Kato, A.; Minoshima, Y.; Yamamoto, J.; Adachi, I.; Watson, A. A.; Nash, R. J. *J. Agric. Food Chem.* **2008**, *56*, 8206-8211.
- (22) Salazar-Gómez, A.; Ontiveros-Rodríguez, J. C.; Pablo-Pérez, S. S.; Vargas-Díaz, M. E.; Garduño-Siciliano, L. S. *Afr. J. Bot.* **2020**, *135*, 240-251.
- (23) Zhu, F.; Li, X. X.; Yang, S. Y.; Chen, Y. Z. *Trends Pharmacol. Sci.* **2018**, *39*, 229-231.
- (24) Discovery Studio. Discovery Studio Life Science Modeling and Simulations; Accelrys, 2008.
- (25) Daina, A.; Michielin, O.; Zoete, V. *Sci. Rep.* **2017**, *7*, 42717
- (26) Lipinski, C. A.; Lombardo, F.; Dominy, B. W.; Feeney, P. J. *Adv. Drug Deliv. Rev.* **2001**, *46*, 3-26
- (27) Khaerunnisa, S.; Suhartati, S.; Awaluddin, R. Penelitian In Silico untuk Pemula; Airlangga University Press: Indonesia, **2020**, pp 67-89
- (28) Kousaxidis, A.; Petrou, A.; Lavrentaki, V.; Fesatidou, M.; Nicolaou, I.; Geronikaki, A. *Eur. J. Med. Chem.* **2020**, *207*, 112742.
- (29) Hajizadeh-Sharafabad, F.; Varshosaz, P.; Jafari-Vayghan, H.; Alizadeh, M.; Maleki, V. *Complement. Ther. Med.* **2020**, *48*, 102284.
- (30) Saeidnia, S.; Manayi, A.; Gohari, A. R.; Abdollahi, M. *European J. Med. Plants* **2014**, *4*, 590-609.
- (31) Ponnulakshmi, R.; Shyamaladevi, B.; Vijayalakshmi, P.; Selvaraj, J.

Toxicol. Mech. Methods **2019**, *29*, 276-290.

(32) Wang, J.; Huang, M.; Yang, J.; Ma, X.; Zheng, S.; Deng, S.; Huang, Y.; Yang, X.; Zhao, P. *Food Nutr. Res.* **2017**, *61*, 1364117.

(33) Reza, M. S.; Shuvo, M. S. R.; Hassan, M. M.; Basher, M. A.; Islam M. A.; Naznin, N. E.; Jafrin, S.; Ahmed, K. S.; Hossain, H.; Daula, A. F. M. S. U. *Biomed. Pharmacother.* **2020**, *132*, 110942.

(34) Hannan, M. A.; Sohag, A. A. M.; Dash, R.; Haque, M. N.; Mohibbullah, M.; Oktaviani, D. F.; Hossain, M. T.; Choi, H. J.; Moon, I. S. *Phytomedicine* **2020**, *69*, 153201.

(35) Wianowska, D.; Gil, M. *Phytochem. Rev.* **2019**, *18*, 273-302.

(36) Chen, L.; Teng, H.; Cao, H. *Food Chem. Toxicol.* **2019**, *127*, 182-187.

(37) Du, X.; Li, Y.; Xia, Y. L.; Ai, S. M.; Liang, J.; Sang, P.; Ji, X. L.; Liu, S. Q. *Int. J. Mol. Sci.* **2016**, *17*, 144.

(38) Patil, R.; Das, S.; Stanley, A.; Yadav, L.; Sudhakar, A.; Varma, A. K. *PLoS ONE*, **2010**, *5*, 1-10.

(39) Talbot, E. P. A. Towards the synthesis of anthecularin and anthecotulides; Faculty of Physical Sciences, University of Oxford: United Kingdom, **2011**, pp 1-8.

(40) Chaturvedi, D.; Dwivedi, P. K. In *Discovery and Development of Antidiabetic Agents from Natural Products: Natural Product Drug Discovery*; Brahmachari, G. Ed; Elsevier Inc; USA, **2017**, pp 185-207.

(41) Bule, M.; Abdurahman, A.; Nikfar, S.; Abdollahi, M.; Amini, M. *Food Chem. Toxicol.* **2019**, *125*, 494-502.

(42) Jaishree, V.; Narsimha, S. *Biomed. Pharmacother.* **2020**, *130*, 110561.

(43) Eid, H. M.; Haddad, P. S. *Curr. Med. Chem.* **2017**, *24*, 355-364.

(44) Ali, M. Y.; Jannat, S.; Rahman, M. M. *Comput. Toxicol.* **2020**, *17*, 100141

(45) Li, L.; Luo, W.; Qian, Y.; Zhu, W.; Qian, J.; Li, J.; Jin, Y.; Xu, X.; Liang, G. *Phytomedicine* **2019**, *59*, 152774.

(46) Lin, Y.; Liu, P. G.; Liang, W. Q.; Hu, Y. J.; Xu, P.; Zhou, J.; Pu, J. B.; Zhang, H. J. *Phytomedicine* **2018**, *41*, 54-61.

(47) Lodhi, S.; Vadnere, G. P.; Patil, K. D.; Patil, T. P. *J. Tradit. Complement. Med.* **2020**, *10*, 60-69.

(48) Addepalli, V.; Suryavanshi, S. V. *Biomed. Pharmacother.* **2018**, *108*, 1517-1523.

(49) Ma, Y.; Ding, S.; Fei, Y.; Liu, G.; Jang, H.; Fang, J. *Food Control* **2019**, *106*, 106712.

(50) Bursal, E.; Taslimi, P.; Gören, A. C.; Gülçin, İ. *Biocatal. Agric. Biotechnol.* **2020**, *28*, 101711.

(51) Saeidnia, S.; Abdollahi, M.; *Toxicol. Appl. Pharmacol.* **2013**, *273*, 442-455.

Received January 14, 2021

Revised April 21, 2021

Accepted April 25, 2021